LIMNOLOGY
and
OCEANOGRAPHY: METHODS

Limnol. Oceanogr.: Methods 6, 2008, 64–80

A large-volume microfiltration system for isolating suspended particulate organic matter: fabrication and assessment versus GFF filters in central North Pacific

Leslie A. Roland[1], Matthew D. McCarthy[1], Tawnya D. Peterson[2], and Brett D. Walker[1]*

[1]Department of Ocean Sciences, University of California, 1156 High Street, Santa Cruz, CA 95064, United States

[2]Science & Technology Center for Coastal Margin Observation & Prediction, Oregon Health and Science University, Beaverton, OR 97006

Abstract

We describe the construction and testing of a home-built ultrafiltration (UF) system, based on commercially available hollow fiber polysulfone membranes, for isolation of suspended particulate organic matter (POM_{susp}) from large volumes (2000–10,000 L) of ocean water. The overall apparatus consists of two sequential UF steps: a main filtration system (100 L reservoir) driven by a stainless steel centrifugal pump, and a subsequent reduction/diafiltration system (2 L reservoir) driven by a peristaltic pump. The system can be readily assembled using off-the-shelf parts at a fraction of the cost of commercial UF systems. Our system functioned comparably to previously described commercial units. We conducted a series of tests using both surface (21 m) and mesopelagic (674 m) N. Pacific central seawater from ocean pipeline sources at the Natural Energy Laboratory Authority of Hawaii (NELHA), while simultaneously collecting GFF-POM samples. We evaluated flow rates, fouling behavior, carbon and nitrogen recoveries and compositions, and also bacteria and virus retention of ultrafiltered-POM (UPOM) using both 0.1 μm and 500 kilodalton pore size membranes. We also compared composition of UPOM versus GFF-POM, finding clear differences, which also varied between surface and mesopelagic waters. Finally, to evaluate the appeal of large-volume filtrations at NELHA to study central N. Pacific Gyre POM_{susp}, we compared our data with offshore station ALOHA.

Introduction

Particulate organic matter (POM) represents one of the largest dynamic carbon reservoirs in the ocean. Sinking POM is a source of regenerated nutrients that support primary productivity, hetetrophic life in the subsurface, and ultimately represent the major removal pathway for atmospheric CO_2 (Lee et al. 2005; Suess 1980; Wakeham et al. 1997). Whereas sinking POM is a key component of the ocean carbon cycle, the larger proportion of the total POM pool exists suspended in the water column (Lee et al. 2005; McNichol and Aluwihare 2007; Megens et al. 2002). Whereas suspended and sinking POM are linked to some extent via aggregation/disaggregation processes (Alldredge and Jackson 1995; McCave 1984), POC_{susp} has distinct chemical and isotopic compositions relative to its sinking counterpart (Druffel et al. 1998; Repeta 1984; Wakeham and Ertel 1988). Microbial loop processes have a large effect on the POC_{susp} pool by mediating carbon, nutrient, and metal transfers between particulate and dissolved phases (Clegg et al. 1991; Shaw et al. 1998). Finally, because POC_{susp} is primarily advected with water masses, its persistence and ultimate degradation consists of very different linkages in the ocean carbon cycle in comparison to sinking POM (Bauer and Druffel 1998). Understanding POM_{susp} preservation and degradation processes are therefore central to global carbon and nitrogen cycle dynamics.

Despite substantial scientific interest in the sources and cycling of POM_{susp}, the collection of sufficient material for detailed organic chemical analyses is challenging. GFF filters are widely used for collection of POM_{susp}, typically allowing material to be isolated from 1–10 L of seawater. While suitable

*Corresponding author: E-mail: mccarthy@pmc.ucsc.edu
Tel.: + 1-831-459-1533

Acknowledgments

This work would not have been possible without the dedication and enormous assistance from Jenny Lehman, Ian Voparil, and Ian Hewson. In addition, generous support in all aspects of logistics and sampling by staff at the Natural Energy Laboratory of Hawaii Authority (NELHA) facility was key for our large-volume filtrations. We also would like to thank Dan Repeta at WHOI for generous ideas regarding home-built UF design. Funding was provided by University of California, UCOP campus-laboratory collaborations and the National Science Foundation. The paper benefited greatly from the comments of three anonymous reviewers.

for many bulk geochemical studies (e.g., elemental ratios, stable isotopes, etc), standard GFF-POM isolations cannot yield enough material for many molecular-level techniques. Large volume (100–10,000 L) isolations through larger pore-size filters (0.8–1 μm) using in situ pumps (e.g., Bishop et al. 1977; Druffel et al. 1998) have been developed to address the problem of sample size, allowing molecular-level organic analysis (e.g., Lee et al. 2000; Minor et al. 1998; Wakeham and Canuel 1988). However, techniques in which particles become embedded in a filter matrix present inherent problems for many analyses, especially techniques requiring a relatively pure organic sample (e.g., solid-state NMR, pyrolysis), while acid hydrolysis can produce inorganic byproducts that cause problems with subsequent derivatization reactions required in many molecular-level analyses.

Recently, tangential-flow ultrafiltration (UF) has been applied to filter large volumes of seawater for the collection of $POM_{susp,}$ allowing a wider variety of organic techniques to be applied to study origin, cycling, reactivity, and composition (Benner et al. 1997; Hernes and Benner 2002; Sannigrahi et al. 2005). UF is a method in which fluid flows tangential to the filter surface (e.g., Cheryan 1998) and is recirculated at constant pressure across the membrane, such that components smaller than the nominal molecular weight cut-off (NMWCO) pass the membrane, whereas larger components are progressively concentrated in the "retentate" reservoir. If operated at appropriate recycle rates and pressures, membrane clogging is minimal, and thus very large volumes can be processed. UF systems with hollow fiber type membranes (sometimes referred to as "cross-flow" hollow fiber systems) are commonly used in the biomedical industry. For marine applications, isolated materials are directly desalted by cycling deionized water (DI) as a final step through the system (e.g., Benner et al. 1997).

Previous isotopic and chemical studies of ultrafiltered POM (UPOM) composition (Benner et al. 1997; Hernes and Benner 2002; Sannigrahi et al. 2005) used polysulfone hollow fiber UF membranes at 0.1 μm NMWCO on a commercial ultrafiltration system (Amicon DC 10L). However, due to industry changes, these systems and membranes they used are no longer available. Other large-scale commercial hollow fiber systems designed for biomedical applications remain available (e.g., GE Biosciences/Amersham "*grandstand"* line), however at costs prohibitive to many academic research groups (~US$80,000 as of 2007). While the development of small-scale UF apparatuses have been described for specific experiments (e.g., Powell and Timperman 2005), fabrication of appropriate large-volume systems has never been detailed, and tests of currently available membranes have never been published for marine POM_{susp}.

We describe here the fabrication and testing of a home-built, semi-automated UF system for collection of marine POM_{susp}. The two-stage system is designed to process 100-10,000 L seawater samples to a final desalted volume of ~1 L. The system was built around commercially available hollow fiber membranes (GE Biosciences/Amersham), and "off-the-shelf" centrifugal pumps, plumbing, reservoirs, and electronic controllers, with total costs a fraction of analogous commercial systems. To examine performance relative to commonly reported marine POC data, we compared POM_{susp} carbon recovery, elemental ratio, and stable isotopic compositions relative to standard GFF filters in both near-surface (21 m) and mesopelagic (674 m) central Pacific waters using 0.1 μm versus 500 kilodalton (kD) UF membranes. We also tested relative retention of bacteria and viruses, and examined larger phytoplankton for evidence of cell collapse or lysis during long recirculation times. Finally, our sampling site at the National Energy Laboratory of Hawaii Authority (NELHA) in the north central Pacific gyre permits comparison of our collected POM_{susp} relative to earlier work using UF at nearby station ALOHA (Benner et al. 1997; Hernes and Benner 2002; Sannigrahi et al. 2005), and is directly applicable to both past and ongoing research projects using this same water source (e.g., Ingalls et al. 2006; Repeta and Aluwihare 2006).

Materials and procedures

Sampling site—Seawater samples were collected from the big island of Hawaii near Kailua-Kona (19°69´N, 156°03´W), at NELHA (http://www.nelha.org/about/facilities.html) in December 2005. Large diameter pipes placed on a steep volcanic escarpment bring very high seawater flows (36,000-50,000 L/min) to the surface from depths of 21 m, 674 m, and 900 m. The station is located on an undeveloped lava field on the "desert" side of the big island of Hawai'i, and has no terrestrial freshwater sources. Water from this location has been declared unaffected by anthropogenic influences and representative of local tropical ocean water by the Hawaii State Department of Health. Due to the essentially unlimited access to mesopelagic central Pacific water at NELHA, several POM and dissolved organic matter (DOM) studies have been conducted at this site; these have indicated that studied aspects of POM and DOM isolated from NELHA are comparable to those in the central North Pacific gyre (Ingalls et al. 2006; Repeta and Aluwihare 2006).

System description—Fig. 1 and Table 1 show a detailed schematic and component summary list of our dual sequential UF systems. First, a main (large-volume) concentration system, using a 110-L reservoir and driven by a 1.5 HP centrifugal pump (Fig. 1a), and a second, small-volume, reduction/diafiltration system, using a 2-L reservoir and driven by a 1/8 HP peristaltic pump (Fig. 1b). An aluminum cage (not shown in Fig. 1) supports both systems. For the main isolation system, we also included fluid level-control automation, which greatly facilitated processing of large volumes.

System fill and automation—Source fluid consisted of constantly flowing seawater from the NEHLA pipes, which were directed into a 20-L polycarbonate carboy fitted with a 50 μM mesh Nitex® plankton netting, to exclude larger organisms or detritus. The <50 μm filtered seawater was transferred by an

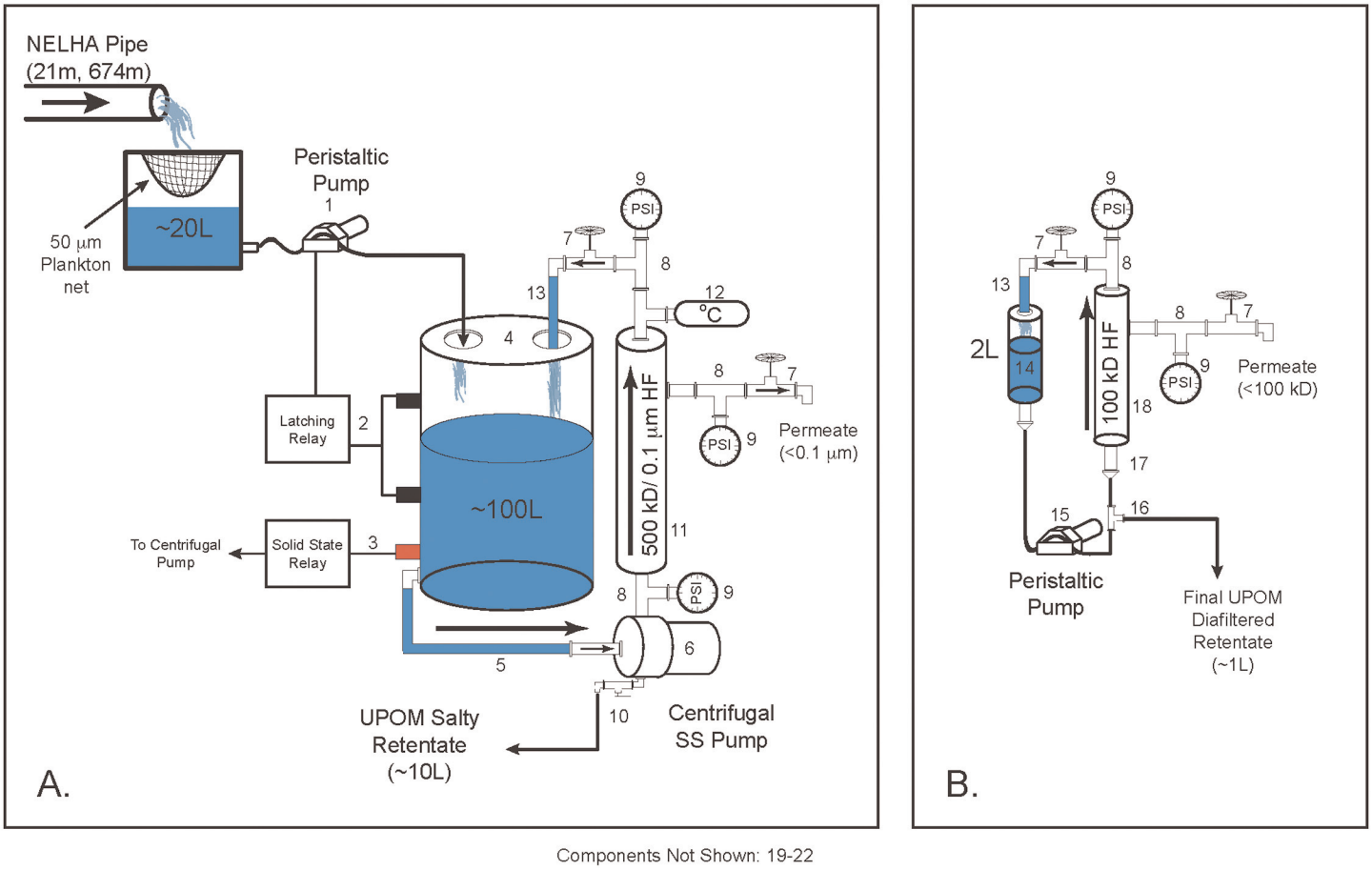

Fig. 1. Schematic of UPOM concentration and reduction systems. Features and operation are described in the *Methods* section. Numbers refer to specific components listed in Table 1, or discussed in text. A) Main system, consisting of a 100-L reservoir, large (0.5-1.5 HP) centrifugal pump, and 500 kD or 0.1 µm membrane; minimum working volume of ~10 L. B) Reduction/Diafiltration system, consisting of 2 L reservoir, 1/8 HP peristaltic pump, and 100 kD membrane; minimum working volume ~1 L. Actual systems were mounted on support cages constructed from aluminum strut channel (not shown, components #18-21 in Table 1), as described in text.

automated "feed pump" into the main system reservoir via a 1/8 HP peristaltic pump (Masterflex I/P) and silicone tubing (1N HCl/Milli-Q water cleaned). Two non-intrusive RF capacitance sensor relays were mounted on the exterior of the fill reservoir at both 60% and 80% tank level, and were coupled to a level controller/latching relay (OMEGA) to maintain a consistent tank volume (Fig. 1a, nr 2). We also tested a more basic automation using stainless steel float switches. In addition, a "fail-safe" solid-state relay (Fig. 1a, nr 3) was installed, linked to a proximity level sensor (OMEGA and Cole-Parmer) located near the tank bottom. This second relay acted as a "kill switch" to turn off all pumps if the fill automation failed, and to prevent the tank running dry.

Main concentration system: 500 kD versus 0.1 µm—Fluid was recirculated within the fill reservoir via 1-inch ID Teflon® corrugated tubing and a centrifugal pump with 316 stainless steel pump head. For most isolations, we used a 1.5 HP pump (G&L Model #: 1ST1F2B4, max RPM = 3600), but we also tested a smaller 0.5 HP model (G&L Model #: 1ST2C2A4, max RPM = 1750). Pumps were driven by a variable-speed AC controller (AC Tech, MC Series). Typical drive settings ranged from 40-60 Hz (where 60 Hz = max RPM). A temperature probe was placed after the membrane. Pressure gauges (0-30 PSI) were placed before and after the membrane, and also at the permeate port (Fig. 1). We monitored recycle fluid temperature, transmembrane pressure (TMP), and system backpressure during isolations. Fluid recycle rates were measured manually to determine fluid shear rate (discussed below), and the system was calibrated for recycle rate versus pump speed.

We tested two pore size 2.1 m^2 hollow fiber polysulfone membranes from GE Biosciences/Amersham: 500 kD NMWCO (UFP-500-E-55) and 0.1 µm (CFP-1-E-55), both with the largest available lumen diameter (1 mm), in 7.6 × 60 cm polysulfone housings. The bottom side-port was sealed during filtration, while the top side-port was fitted with an open/close permeate valve. At system startup, the top side-port was left open until water reached the top of the membrane; after which the permeate valve was closed and the

Table 1. Summary component list for UPOM filtration systems

Part Nr*	Component description	Supplier
1	Peristaltic Pump - High Capacity Pump Controller and Motor (50/60Hz), Masterflex I/P	Cole-Parmer
1	Pump Head, Polysulfone Housing, Stainless Steel Rotor	Cole-Parmer
2	Dual Sensor Level Controller, Latching Relay (LCVN-130)	OMEGA Engineering
2	316 SS Liquid Level Switches (LV-40)	OMEGA Engineering
2	Solid State Latching Relay (SSRL)	OMEGA Engineering
2	RF capacitance sensor relays, non-intrusive (LVP-51-R)	OMEGA Engineering
3	High-Reliability Solid State Relay (SSRL240)	OMEGA Engineering
3	Proximity Switch, non-contact	Cole-Parmer
4	HDPE Tank with Spigot, 114L, Nalgene	Fisher Scientific
5	PTFE Corrugated Tubing, 1" ID, 3 ft.	McMaster-Carr
6	316 SS Centrifugal Pump, G&L Model #1ST1F2B4, 1.5 HP	Albany Pumps
6	316 SS Centrifugal Pump, G&L Model #1ST2C2A4, 0.5 HP	Albany Pumps
6	MC Series AC Inverter, AC 115V IN - 230V OUT	Albany Pumps
7	316 SS Globe Valve, 1" NPT or 1/2" NPT	McMaster-Carr
8	316 SS Quick-Clamp Sanitary "T" Fitting, 1.5" Tube OD	McMaster-Carr
9	316 SS Sanitary Pressure Gauges, 0-30 PSI	McMaster-Carr
10	316 SS Ball Valve, 3/8" NPT	McMaster-Carr
11	500 kD HF Membrane, UFP-500-E-55, 2.1m^2	GE Biosciences
11	0.1 μm HF Membrane, CFP-1-E-55, 2.1m^2	GE Biosciences
12	Solar Digital Vari-Angle Thermometer (F), with 2" Probe	CA Hydronics
13	Teflon® PTFE Tubing, 1" ID, 2 ft.	McMaster-Carr
14	2L Polysulfone Reservoir w/ Sealable Top (56-4107-67)	GE Biosciences
15	Peristaltic Pump Controller and Motor (115/230V), Masterflex I/P	Cole-Parmer
15	Pump Head, Polysulfone Housing, Stainless Steel Rotor	Cole-Parmer
16	PVDF 3-Way, Elliptic Valve	Cole-Parmer
17	PVDF Sanitary Barbed Adapter	Cole-Parmer
18	100 kD HF Membrane, UFP-100-E-8A, 3600cm^2	GE Biosciences
19	Al Single Strut Channel Slotted, (1-5/8" × 1-5/8") and (1-5/8" × 13/16")	McMaster-Carr
20	304 SS Strut Channel Braces	McMaster-Carr
21	316 SS 3/8" Hex Screws	McMaster-Carr
22	Teflon® PTFE Sanitary Gasket, 1.5" DIA	McMaster-Carr

*Part Nr refers to numbered components in Fig. 1 schematic, SS = stainless steel; HF = hollow fiber

system was primed for ~10 min, followed by draining all water from the system, before re-opening the permeate valve to begin filtration. Retentate volume was manually reduced to < 10 L before transfer to the reduction/diafiltration system.

100 kD reduction/diafiltration system—Our reduction system was designed to reduce volumes to ~1 L of desalted (diafiltered) retentate. Volumes of this size facilitate drying and further processing in the lab, but also can be more practically stored frozen and transported. This system was driven by a 1/8 HP peristaltic pump (Cole-Parmer, Masterflex I/P), plumbed with acid-cleaned silicon tubing. It used a 2 L polysulfone reservoir and a 3600 cm^3, 100 kD MWCO polysulfone HF membrane with 1mm lumen diameter (GE Biosciences/Amersham; UFP-100-E-8A) in a 5.1 × 30 cm polysulfone housing. A Teflon 3-way valve (Cole-Parmer) was fitted between the pump and membrane for collection of final retentate. Pressure gauges (0-30 PSI) were placed at the top side-port and the membrane intake to monitor permeate pressure and back pressure. After UPOM retentates were reduced, they were diafiltered with 6 L Milli-Q water, or until salinity reached zero (via portable refractometer). Final desalted UPOM retentates were frozen in the field, transported to the lab in Santa Cruz where they were dried via lypholization or centrifugal evaporation, homogenized by mortar and pestle, and stored for analysis.

Operating conditions—Key operating variables for hollow fiber UF systems are transmembrane pressure (TMP) and fluid shear rate (Amersham Biosciences 2004; Cheryan 1998). Table 2 describes pump settings, recycle flow rates, and pressures, as well as the resulting fluid shear conditions tested. Filtration shear rates ($r = s^{-1}$) are expressed as a ratio of fluid velocity (q) versus membrane lumen radius (R):

$$r = (4q)/\pi R^3 \quad (1)$$

Lumen radius strongly affects shear, however our membranes all had identical large lumen ID, which is least susceptible to membrane fouling (Cheryan 1998). Therefore, relative

Table 2. Operating parameters for UPOM system tests*

UPOM nr	Depth	Membrane	Temp (°C)	Open perm. flow?	Pump speed (Hz)		Recycle flow rates† (L/min)		Back-pressure§ (PSI)		Perm-out pressure¶ (PSI)		Trans-membrane pressure#	Shear rate (s^{-1})		Perm. flow rate (L/min, mL/min)		Total volume filtered** (L)
					500/0.1††	100††	500/0.1††	100††	500/0.1††	100††	500/0.1††	100††	500/0.1††	500/0.1††	100††	500/0.1††	100††	
3	21	500 kD	26-27	N	60	40%	78	7	6.0	0.5	3.0	0	5.5	~11,500	7200	3.3	120	4950
4	21	500 kD	26-27	Y	40	40%	42	7	2.0	0.5	0	0	3.5	~6000	7200	2.6	120	3672
6	21	0.1 μm	25-27	Y	25	40%	60	7	2.5	0.5	0	0	5.5	~8000	7200	5.0	160	5130
1	674	500 kD	10-13	N	60	40%	78	7	4.5	0.5	3.5	0	4.5	~11,500	7200	2.5	160	3600
2	674	500 kD	8-10	Y	40	40%	42	7	2.0	0.5	0	0	3.5	~6000	7200	2.1	130	4536
7	674	500 kD	9	Y	60	40%	90	7	7.5	0.5	0	0	8.0	~12,000	7200	3.2	140	9158
5	674	0.1 μm	9-10	Y	25	40%	60	7	2.0	0.5	0	0	5.5	~8000	7200	5.1	120	8319

*UPOM system operating conditions for each test, including pump speeds (Hz) and valve conditions, and resulting shear rates.
†Stream flow is the recirculation flow rate through the system, §backpressure is the pressure at the membrane outlet (P_{out}), ¶permeate pressure is pressure measured at the permeate valve, and #transmembrane is calculated as explained in text. These quantities are discussed in *methods* section.
**Total volume filtered refers to the total sample size for a given test.
††Designation "500/0.1" and "100" indicate membrane size(s) used for a given set of conditions.

shear rates in our experiments were determined by fluid recirculation speed, because for a given lumen diameter shear increases linearly with flow.

TMP is defined as the pressure gradient across the membrane:

$$TMP = [(P_{in} + P_{out})/2] - P_{perm} \quad (2)$$

P_{out} is the "outlet" pressure of the fluid leaving the membrane, also referred to as "backpressure." P_{in} is the membrane "inlet" pressure, and P_{perm} is the pressure of the permeate, defined as fluid which passes the membrane (< 0.1 μm or < 500 kD). Flow rate, TMP, and permeate flow rates are controlled by adjusting pump speed and system backpressure (Fig. 1). Under typical operating conditions TMP pressures were ~5 PSI, never exceeding 10 PSI, while backpressure values ranged from 2-8 PSI.

The 500 kD membrane was tested in both surface and mesopelagic water at high and intermediate shear conditions (Table 2). For high shear conditions, UPOM isolations were performed at maximum pump speeds (60 Hz, 3600 rpm) with a controlled permeate flow of ~3 L/min (P_{perm} = 3-3.5 PSI). Recirculation rates were ~80 L/min, resulting in a shear rate of 11,500 s^{-1}. TMP and backpressure values were similar, near 5 PSI. For intermediate shear rate tests, the pump was run at 40 Hz, but with a fully "open" permeate flow (~2.3 L/min; P_{perm} = 0 PSI). The recirculation rate was ~40 L/min, resulting in shear rate of 6000 s^{-1}. Both TMP and backpressures were lower than in the high shear tests (3.5 and 2 PSI, respectively). We also carried out one very large volume (9150 L) mesopelagic-water isolation at high shear (~12,000 s^{-1}) using maximum pump speeds (60 Hz) and an open permeate flow (3.2 L/min; P_{perm} = 0 PSI). Recirculation rates reached ~90 L/min, and TMP and backpressures were highest (9.5 and 7.5 PSI, respectively).

The 0.1 μm hollow fiber membrane was tested at only a single shear rate (~8000 s^{-1}) in surface and mesopelagic water. The 0.1 μm tests used a 0.5 HP G&L pump, run at intermediate pump speed (25 Hz out of 30 Hz max) with a high permeate flow (5 L/min; P_{perm} = 0 PSI). Recirculation flows were ~60 L/min, with TMP and backpressures of 5 and 2.5, respectively.

All UPOM samples were reduced and diafiltered under the same shear conditions using a 100 kD hollow fiber filter. We used an intermediate pump speed and open permeate port (Perm. Flow = 120-160 mL/min; P_{perm} = 0 PSI) to minimize potential cell damage. This membrane had recirculation flow rates of ~7 L/min, with a shear rate of 7,200 sec^{-1}. TMP was not measured during diafiltration, but backpressure was ≤ 0.5 PSI for every sample diafiltered.

Membrane cleaning—Membranes were first flushed with 100 L DI water, followed by cycling 20 L DI at full pump speed until fluid was warm (24-27°C, ~ 1 h). Next, a 0.5N NaOH (20 g/L) solution was circulated for 1-2 h, and the membrane was soaked in this basic solution overnight. Finally, membranes were rinsed with 100 L Milli-Q or until neutral pH. A full cleaning protocol was used between tests on different water

sources (21 and 674 m), while a truncated cleaning protocol was used between replicate filtration tests conducted from identical waters: two 30 min cycles/flushes with 20 L Milli-Q (or until clear), followed by a 60 L UDOM permeate cycle and flush (1 h). To test for fouling, reference measurements of recirculation and permeate flow rates for particle-free seawater (<1000 kD permeate from a separate UF system) were made at the start of field experiments, and cleaning was continued until values returned to initial levels. For long-term storage, clean membranes are kept refrigerated in weak NaOH.

Sampling and microscopy for plankton, bacteria, and viruses—Prior to diafiltration, subsamples were taken to evaluate phytoplankton species composition and physical condition, and also bacterial and viral counts. Samples for light microscopy (200 mL) were preserved with 1% Lugols Iodine solution and stored at 4°C in the dark. The preserved material was settled in Utermöhl settling chambers within a month of collection (Hasle 1978; Utermöhl 1958) and counted on a Zeiss Axioskop inverted microscope at 400 × magnification. A minimum of 300 cells per sample was enumerated. Bacteria and virus samples were flash-frozen in a EtOH/dry ice slurry, stored in polypropylene BD50 Falcon conical tubes preserved with 2% vol:vol formaldehyde solution (0.2 μm pre-filtered), and stored at –80°C until analysis. After dilution, counts were performed following the SYBR Green 1 protocol of Noble and Fuhrman (1998) filtered through 0.02 μm Anodisc filters and visualized under blue light excitation at appropriate magnification. A minimum of 200 cells per sample was counted. Even though bacteria form aggregate "clumps" after diafiltration, they were still counted in the same manner of 200 cells but required less fields.

GFF-POM and UPOM elemental and isotopic measurements—Approximately 8 L of source seawater was pressure-filtered (10-15 PSI) through precombusted 0.7 μm GFF filters to determine POM recoveries and isotopic values. Filters were dried at 50°C and vapor acidified with 12N HCl following methods described by Hedges and Stern (1984) prior to elemental and isotopic analyses to remove potential carbonates.

Total organic carbon (TOC), total nitrogen, $(C/N)_a$ ratios and stable C ($\delta^{13}C$) and N ($\delta^{15}N$) isotopic measurements were determined on all UPOM fractions, however $\delta^{15}N$ values could not be determined accurately for GFF samples due to low total nitrogen. Isotopic and elemental measurements were made at UCSC light stable isotope facility using a Carlo Ebra CHNO-S EA-1108 Elemental Analyzer coupled to a Thermo-Finnigan Delta Plus XP continuous flow isotope ratio mass spectrometer (EA-IRMS) system. Values were standardized to PeeDee Belemnite and atmospheric N. Reproducibility of analyses was ± 0.1‰ for $\delta^{13}C$ and ± 0.6‰ for $\delta^{15}N$.

TOC values of selected UPOM liquid retentates were also measured to assist in estimating total carbon balances. Samples for TOC were recovered from 1) net-filtered source waters, 2) main UPOM concentrates and 3) final diafiltered UPOM retentate. Retentate samples were collected directly into muffled glass vials with acid-cleaned Teflon-lined caps and immediately frozen. TOC analyses were performed in constantly bubbled (mixed) vials, via a high-temperature combustion TOC analyzer (Shimadzu TOC-V) at the University of California, Santa Barbara marine analytical facility.

Assessment

UPOM system performance, quantity, and composition was evaluated under varying operating conditions with volumes ranging from 3600-9200 L, in surface (21 m) and mesopelagic (674 m) water sources, under two contrasted shear conditions. We also tested both 500 kD and 0.1 μm membranes. Whereas a 0.1 μm pore size corresponds most closely with commonly defined oceanic POC, all UF membrane pore sizes are nominal, and the manufacturer (GE Biosciences/Amersham) advises using a membrane NMWCO several ranges *smaller* than the smallest particles targeted for full retention, especially when using high concentration factors. Our main assessment goals were to test overall system performance and to examine the composition of isolated UPOM compared with GFF-collected material, using our different configurations and operating conditions.

Overall design and performance—We evaluated our physical configuration for ease of use and robustness in the field. In general, the system described (Fig. 1, Table 1) performed very well. Several aspects of our design warrant brief discussion.

Cage and supports—The aluminum strut channel cage was robust, easily supporting the system. This material is inexpensive, easy to assemble and modify in the field, and we found it far superior to expensive, custom-welded supports that we have used previously.

Pumps—The stainless-steel centrifugal pumps that we tested for our main concentration systems were effective, robust, and relatively inexpensive. Key pump criteria include 1) sufficient power to operate specific membranes under target pressure/shear conditions, 2) relatively pulse-free flow, 3) pump components that will not contaminate the sample, and 4) lack of cell damage to delicate samples. However, the smaller pump we tested (0.5 HP) could operate only the 0.1 μm membrane at target conditions. A larger motor size allows more flexibility, and also for several membranes to be operated in parallel if desired. For our reduction system, the 1/8 HP peristaltic pump worked well. A peristaltic pump for smaller systems is one of the configurations recommended by our membrane manufacturer (GE Biosciences/Amersham), and plumbed with replaceable Si tubing proved easy to operate and clean.

Level-control automation—This enabled the processing of large sample volumes. The nonintrusive RF capacitance sensors that we tested proved to be less reliable than the simple stainless steel liquid float switches. These "proximity" switches worked perfectly in the lab, however in the field they failed on a number of occasions, possibly from the tank condensation associated with cold deep ocean water interfering with calibration. In contrast, the simple stainless steel float

switches operated without incident. Though these must be inserted into the sample fluid, only stainless steel and Teflon actually contact the sample. For the "kill switch" relay at the tank bottom, we felt that proximity switches remained the best option. Although still subject to the issues described above, these are never activated except in case of pump failure, and always held their calibrations in all tests. During long field-trial filtrations the "kill" switch saved our samples in the middle of the night on several occasions.

Permeate flow rates—Permeate flow rate determines sample processing speed, and ultimately the sample volume that can be isolated by a given UF system. Key factors affecting permeate flow rate are membrane size (total surface area), membrane properties (pore size, lumen diameter and length), fluid temperature, ionic strength, and particle load. Our membrane flows in freshwater were consistent with manufacturer specifications, but decreased ~6% for both pore sizes in a seawater matrix (i.e., in particle-free seawater).

In seawater, we experienced working permeate flows of 2-3 LPM with the 500 kD (ultrafilter) membrane and 3-6 LPM with the 0.1 μm (microfilter), allowing 24 h sample sizes of 3500-5000 L in surface water (26°C) and 3500-9000 L in deep water (6°C). These sample volumes could easily be doubled in our system by adding a second membrane in parallel. Compared with previous large volume UPOM isolations (Benner et al. 1997; Hernes and Benner 2002), our system processed larger volumes due to the higher total membrane surface area. Actual permeate flow rates also varied strongly with temperature, shear rate, and TMP, so the exact processing rate will depend strongly on specific sample and run conditions chosen (Fig. 2; Table 2).

Membrane shear and fouling behavior—UF hollow fiber membranes can experience significant permeate flow reduction (and material loss) due to membrane fouling (e.g., Benner et al. 1997; Cheryan 1998). Two independent processes are important: 1) the concentration polarization phenomena (CPP), and 2) irreversible clogging under high particle load conditions (>10% $vol_{particle}$:vol_{reten}; Ghaffour 2004). The CPP is a thin particle layer on the membrane surface (Hong et al. 1997; Song and Elimelech 1995). CPP formation is reversible, and layers can be removed during cleaning. In contrast, irreversible "clogging" consists of particles permanently lodged within pores, even after intensive cleaning methods. It should be noted that the term "fouling" in some technical UF literature is defined as irreversible clogging only. However, in this paper we use "fouling" to encompass all processes that diminish flow rate over time.

Both membrane properties and operating conditions influence susceptibility to fouling. Shear rate is one key variable, with high shear (r = 8000-16,000 s^{-1}) reducing fouling, whereas lower shear rates (r = 4000-8000 s^{-1}) can lead to more rapid flow decrease (e.g., Cheryan 1998). Second, lumen dimension (diameter and length) are both important. Wider lumen diameter decreases clogging problems (Bird et al. 1960),

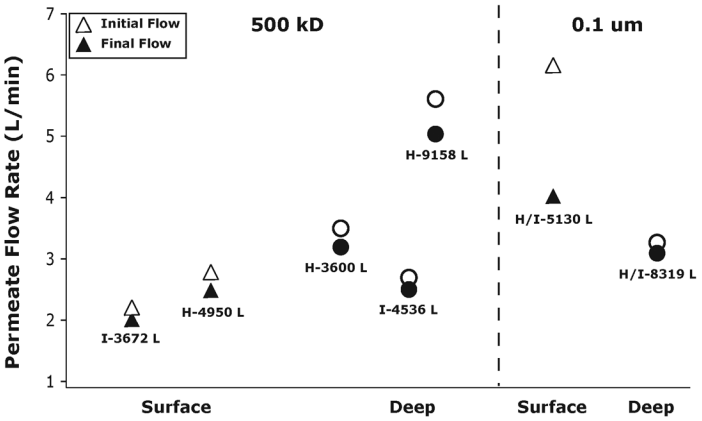

Fig. 2. Relative fouling behavior (permeate flow rate change) versus membrane, water mass, and shear rate. Changes in permeate flow rate (L/min) observed over course of main filtration (large volume) tests indicate relative fouling via CPP layer formation. Tests indicate little fouling with 500 kD membrane or deep water POC, and most significant fouling with surface POC and 0.1 μM membrane. Triangles = surface (21 m) samples, Circles = mesopelagic (674 m) samples; open symbols indicate initial flows and solid symbols indicate final flows. Data are arranged by membrane pore size, and 21 m versus 674 m waters. Total volume filtered for each test is indicated below symbols, as is shear condition used (H = high shear, I = intermediate shear).

but also total filtration surface area. Longer lumen lengths increase surface area, but also increase the pressure drop ($\Delta P = P_{in} - P_{out}$), which in turn promotes clogging (Altmann and Ripperger 1997; Jaffrin et al. 1997). Overall, short length and large diameter membranes should be the least susceptible to fouling, but offer smallest surface area per membrane. Finally, larger membrane pore sizes are more susceptible to both clogging and CPP (Cheryan 1998). In general, as one decreases from what are termed "microfiltration" pore sizes (measured in μm) into "ultrafiltration" pore sizes (measured in kD), the potential for fouling should also decrease (Amersham Biosciences 2004), with smaller size UF membranes typically experiencing no fouling with seawater (e.g., Benner et al. 1997). To isolate the effects of pore size in our tests, we used two membranes (0.1 μm and 500 kD) with identical physical dimensions, both with the largest lumen diameters available.

We monitored permeate flow decreases in our different membranes as a proxy for fouling, over a wide range of filtrate volumes (Fig. 2). Overall, only modest decreases in permeate flow rate was observed in any tests, indicating that membrane fouling was not extensive in oligotrophic ocean waters we tested, even at very high process volumes. Further, after membrane cleaning the permeate flows always returned to initial rates, indicating that the decreases in flow are due to formation of a CPP particle layer. The similar permeate data from both high and low shear conditions also indicate that shear was not a key variable affecting CPP formation in our tests. In particle-rich waters (e.g., coastal or bloom conditions), however, it is likely that these considerations would become more important.

Isolated plankton and potential for cell damage—Cell damage is a possible issue with long UF experiments; in particular if higher cycle flow rates and shear conditions are chosen to minimize fouling. Larger cells (> 5 μm) are sensitive under high shear rate conditions and can be damaged or lysed (Cheryan 1998). Since POM_{susp} (especially in surface waters) is composed in part of intact cells, this could have both a qualitative and quantitative impact: if cells lysed, any dissolved cell material would be lost, decreasing total OC recovered. This could also have more severe consequences in analytical configurations where UPOM isolation is used as a precursor to DOC measurements or HMW DOC isolations (e.g., Benner et al. 1997), since lysed material would become part of the recovered DOC.

We used light microscopy to directly examine the distribution and condition of cells in isolated UPOM (Fig. 3). The UPOM samples contained diverse phytoplankton assemblages in both the surface and mesopelagic samples (Table 3, Fig. 3). Cell abundances were generally low, as is typical for oligotrophic waters, and were approximately 100-fold higher in surface waters (averaging 6.2×10^2 cells/L) than 674 m ($7.0 \times 10°$ cells/L). Surprisingly, many cells at 674 m depth contained intact chloroplasts (Fig. 3d-f). However, the proportion of empty frustules and thecae to living cells was approximately 10 times greater in the mesopelagic samples compared with surface samples. The mesopelagic samples contained many loose coccoliths, particularly belonging to the taxon *Discosphaera tubifera* (trumpet-shaped coccoliths; Fig. 3d). It is notable that the phytoplankton assemblages were mainly composed of several oceanic forms (e.g., coccolithophores such as *Discosphaera tubifera*), but also included some species more characteristic of coastal waters (e.g., *Achnanthes* sp. frustules; Fig. 3f).

Overall, our detailed examinations indicated no detectable cell damage under any shear condition, at any filtration time frame tested. In fact, even delicate structures on coccolithophores and flagellates were clearly preserved in our surface samples (Fig. 3), indicating that our highest shear tests were relatively gentle on algal cells. We conclude that our tested conditions had very minimal impact on the physical integrity of our samples, and in fact that our UPOM system could actually be used to concentrate cells for plankton analysis.

Total POM and UPOM recoveries—

Reported UPOC and UPON concentrations (Table 4) are based on final recoveries of desalted and dried UPOM. We also measured TOC values in the UPOM retentate after the main filtration step, so that we could calculate %UPOM carbon

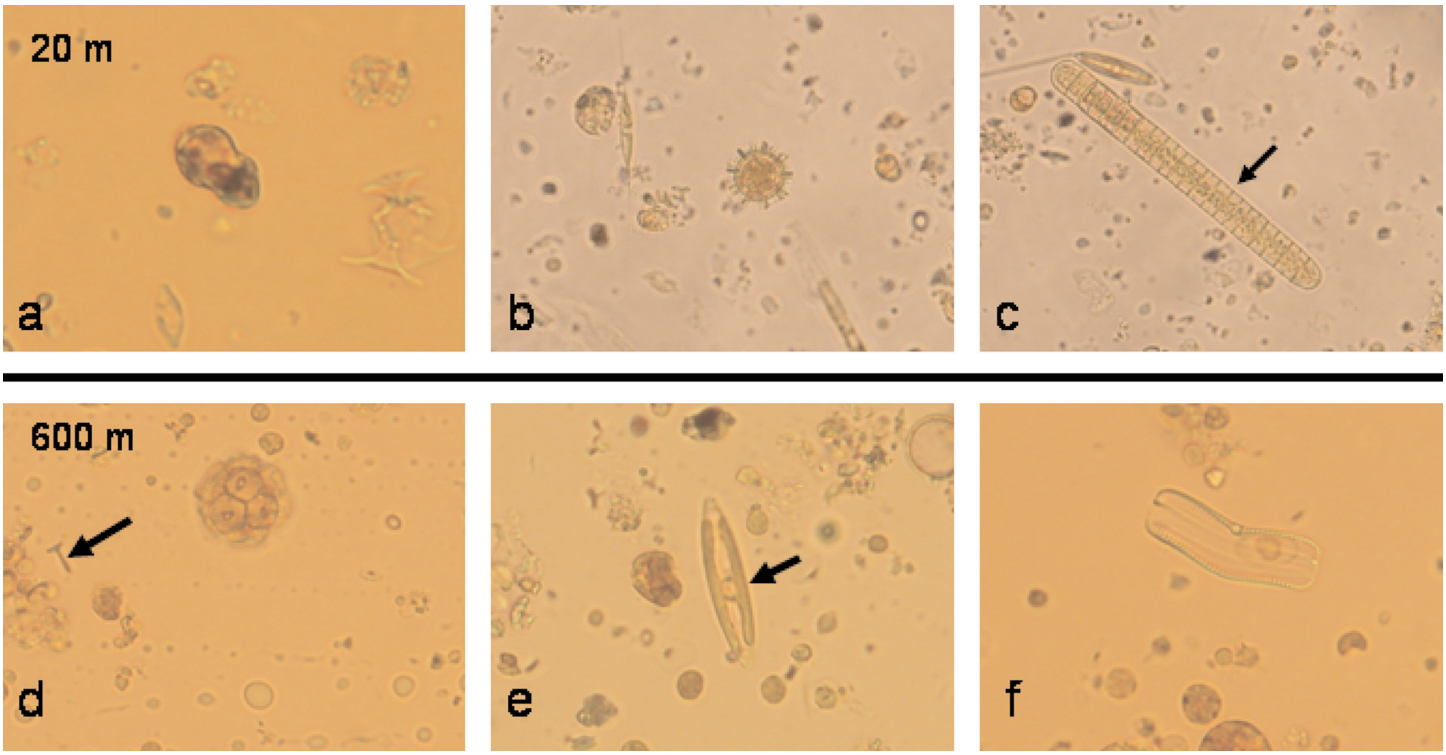

Fig. 3. Selected phytoplankton species images. Micrograph images of microplankton present in samples from 21 m (upper panel) and 674 m (lower panel), showing good condition and intact nature of cells isolated, even after long filtration runs. A) Naked (athecate) gymnodinoid dinoflagellate and empty coccosphere of *Pontosphaera syracusana*, B) intact cells including *Cylindrotheca cylindroformis*, an unidentified pennate diatom, *Pterosperma* sp., and flagellates C) *Trichodesmium* sp. colony, D) coccosphere of *Pontosphaera* sp. and loose coccolith (shown by arrow) of *Discosphaera tubifera*, E) *Navicula* sp. (diatom) with chloroplasts intact, F) empty *Achnanthes* sp. diatom frustule.

Table 3. Major phytoplankton groups and cell abundance*

Taxon	21 m (cells L^{-1})†			674 m (cells L^{-1})†		Surface: deep§
	UPOM 3	UPOM 4	UPOM 6	UPOM 5	UPOM 7	
Diatoms	47	89	125	0.77	0.32	160
Diatom frustules	20	10	24	2	1	13
Dinoflagellates	51	47	88	0.22	1	76
Flagellates	122	448	357	0.33	3	186
Coccolithophores	5	7	9	0.55	2	7
Ciliates	0	0	0	0	0.95	–
Colonial Cyanobacteria	16	98	297	0	0.16	856
Radiolarian	0	0	1	0.11	0	9
Unknown Heterotroph	11	0	2	2	0.63	5
Unknown round balls	0	0	0	156	60	–
Cysts	0	0	0	2	0	–
Amoeba	0	0	1	0	0	1
Silicoflagellate	0	0	1	0	0	1

*Cell concentrations (in cells L^{-1}) of major phytoplankton groups for three samples from the 21-m source (UPOM 3, UPOM 4, UPOM 6) and two samples from 674 m (UPOM 5, UPOM 7). The ratio of cell abundances at 21 m versus 674 m is given for each category, derived from the average abundances for surface (n = 3) and mesopelagic waters (n = 2).
†Values of 0 indicate that no cells were counted
§(Dash) signifies greater concentrations of this species in the mesopelagic than the surface.

losses after main isolation and compare to reduction/diafiltration steps. All UPOM recovery values are compared to GFF-POM values (Table 4).

Surface GFF-POM replicates (n = 3) had average concentrations of 8.3 ± 0.2 μg C/L and 1.1 ± 0.2 μg N/L. Final recoveries from 500 kD isolations at the same depth averaged 3.45 μg C/L and 0.35 μg N/L. TOC measurements indicated that major POC losses occurred during the reduction/diafiltration step. During the main filtration, the 500 kD membrane retained 65% to 83% OC relative to GFF filtration (Fig. 4). After reduction/diafiltration, final UPOC recoveries were 27% to 56% relative to GFF-POM. For the 0.1 μm membrane, surface recoveries were 1.81 μg C/L and 0.25 μg N/L. Whereas 0.1 μm main carbon retention was somewhat lower than 500 kD tests (33% in a single test), the additional retention during the reduction/diafiltration was very similar (67% recovered). Final 0.1 μm membrane surface OC recovery after all steps was 22% (compared with GFF-POC).

Mesopelagic water GFF filters (n = 2) had average concentrations of 5.9 μg C/L (range 5.8-6.1) and 0.6 μg N/L (range 0.5-0.9). Final 500 kD and 0.1 μm membrane recoveries were very similar and averaged 0.38 μg C/L and 0.05 μg N/L, and 0.51 μg C/L and 0.07 μg N/L, respectively. Recoveries after reduction/diafiltration were more variable, however the overall data suggest that in contrast to surface water, only small losses occurred in 674 m samples during reduction/diafiltration. Unfortunately, TOC samples for main retentate with the 500 kD lower shear test (UPOM nr 2) were lost, precluding a direct loss comparison across all conditions. The remaining mesopelagic tests (UPOM nrs 5 and 7) indicated negligible losses during diafiltration and subsequent steps (113% to 125% retained; Table 4). UPOM nr 1 appears to be an outlier with 16% recovery, most likely due to contamination in the main-retentate TOC sample.

UPOM recovery compared to GFF and prior UPOM isolations—Our average GFF-POC concentrations (Table 4) are equivalent to 0.7 μM C in the surface and 0.49 μM C at 674 m, close to expected values for oligotrophic waters. Our final surface UPOC recoveries (22% to 56% relative to GFF) were also generally similar to UPOC recoveries previously reported. Benner and coauthors (1997) reported the only previously published comparison of UPOC versus GFF recoveries. In surface waters, these authors found UF recovered 34% to 64% of corresponding GFF-POC over a wide range of sampling locations, generally similar to our surface water data. However, our mesopelagic UPOM recoveries differed substantially from deep water recoveries in Benner et al. (1997), with these authors reporting nearly quantitative recoveries. In contrast, our mesopelagic UPOM recoveries after diafiltration (5% to 10% versus GFF-POC), were substantially lower than surface water values.

Lower UPOC recovery versus GFF-POC has been attributed primarily to membrane fouling, and in particular, to direct adsorption of material to membrane surfaces (Benner et al. 1997; Powell and Timperman 2005). Our data indicating CPP as the main loss mechanism supports this interpretation. The mechanism is important, as progressive adsorption of material is less likely to result in any total compositional change, as opposed to selective passage of smaller components through the membrane. Reasons for the disparity in our deep water recovery compared with previous work are not clear. One issue is that the much larger surface area membranes we used likely adsorbed a significantly larger proportion of low concentration deep water POM.

Table 4. Sample information, carbon and nitrogen concentrations, elemental and stable isotope ratios, and carbon recovery/mass balance*

Sample information†					Concentration and composition§					Recovery and mass balance¶		
UPOM nr	Depth	Membrane	Shear flow	Conc. factor	μgC/L	μgN/L	$(C/N)_a$	$\delta^{13}C$ (‰)	$\delta^{15}N$ (‰)	Main filtration	Reduc./ diafil.	Overall %C rec.
3	21	500 kD	H	500	2.24	0.24	9.4	–23.4	1.5	65	42	27
4	21	500 kD	I	370	4.67	0.47	9.9	–20.7	1.9	83	67	56
6	21	0.1 μm	H/I	510	1.81	0.25	7.3	–21.2	0.7	33	67	22
1	674	500 kD	H	360	0.29	0.05	6.0	–24.7	4.7	32	16	5
2	674	500 kD	I	450	0.28	0.04	7.2	–23.9	5.8	n.d.	n.d.	5
7	674	500 kD	H	920	0.58	0.07	8.7	–22.0	6.6	8	125	10
5	674	0.1 μm	H/I	830	0.51	0.07	7.4	–22.8	5.0	8	113	9
GFF_{avg}	21	GFF	-	10	8.3 ± 0.2	1.1 ± 0.2	9 ± 2	–24.5 ± 0.3	n.d.	–	–	100
GFF_{avg}	674	GFF	–	10	5.9 ± 0.2	0.6 ± 0.2	12 ± 3	–25.7 ± 0.7	n.d.	–	–	100

*Concentration, composition, and carbon retention versus loss is given for each sample test.
†H = high shear, I = intermediate shear, as per values discussed in text; other standard abbreviations are defined in the text, n.d. = not determined. Conc. Factor = concentration factor for each filtration. Average values for replicate GFF filtrations are reported. Note that GFF errors at 21 m are standard deviation ($n = 3$), but for 674 m are average deviation ($n = 2$).
§UPOM concentrations and composition data reported are based on the final diafiltered and dried retentates.
¶Carbon recoveries (carbon mass balance versus losses to membranes) are given for each filtration step individually, and for the entire process. Main Filtration = % carbon recovery is based on main filtration retentate (TOC versus GFF, ~10 L volume). Reduc./Diafil. = % carbon recovery in retentate after reduction and desalting with 100 kD membrane (~1 L volume) compared with main filtration. Overall %C Rec. = calculated carbon recovery (mass balance) based on total carbon recovered as a dry, desalted powder versus source water GFF. As described in the text, losses are believed to be mainly due to membrane adsorption, via CPP formation.

Fig. 4. Final POC recoveries for GFF versus UPOM filters. Carbon recoveries for GFF filters (black bars), compared to average recoveries using either 500 kD (gray bars) or 0.1 μm (open bar) UF membranes. Mass balance data indicate greater overall carbon recovery in surface versus deep water samples, but also larger losses during diafiltration step with surface POC. Relative carbon retentions are calculated based on defining GFF-POC = 100%. Left panel = 21 m, Right panel = 674 m. Two sets of bars from left to right indicate first average carbon recovery for main (large volume) filtration (retentate ~10 L total volume), and second final values for entire process after the final diafiltration (~1 L total volume), and subsequent sample drying and recovery. Error bars for 500 kD membrane samples represent the total range of carbon recoveries, while 0.1 μm only had one sample at each depth.

Another aspect may be the nature ("stickiness" or surface activity) of particles in given water masses. A general offset in "stickiness" of surface or deep water POM is supported by both Benner et al. (1997) data and our own.

Effects of membrane pore size—A main goal in testing 0.1 μm versus 500 kD membranes was to investigate the effect of pore size. Based on near complete retention of ocean microbes on 0.2 μm flat filters (e.g., Hobbie et al. 1977), a 0.1 μm hollow fiber filter would seem the most appropriate for ocean POC sampling. However, all UF membrane pore size cutoffs are nominal, based on if a single test-solute is > 90% rejected (Cheryan 1998). As mentioned above, technical references, as well as manufacturer recommendations, suggest using a membrane with a nominal pore size a *factor of 10* below the desired particle sizes to be collected (e.g., Cheryan 1998; Zeman and Denault 1992). Based on this rubric, a 500 or 750 kD membrane would be expected to be much more appropriate for complete retention of ocean particles greater than 0.1 μm, with the added advantage of less expected fouling.

In surface water tests, these expectations are borne out, with the 500 kD membrane having substantially higher total POC retention than GFF (Fig. 4; avg = 74%, $n = 2$) under both high and intermediate shear conditions relative to the 0.1 μm membrane (Fig. 4; 33%, $n = 1$). In deep water tests, however, there were no clear differences between 500 kD and 0.1 μm membranes (Fig. 4). Final carbon recoveries after diafiltration (Fig. 4) also indicated increased recovery with 500 kD membranes at 21 m, but similar recoveries for both membranes at 674 m. We suggest that variable

CPP formation might explain these observations, such that particles more prone to clogging (i.e., surface or coastal) would be expected to have a greater retention increase when using a smaller NMWCO filter, which should be less prone to such fouling.

Reduction and diafiltration losses—A main difference between our large-volume system and versions used previously is the necessity for an independent step for sample volume reduction, followed by diafiltration. As indicated above, directly measured losses associate with these two steps indicated they were substantial. Diafiltration of HMW-DOM is also associated with substantial losses, at times approaching 50% (Benner and Eadie 1991; Guo et al. 1994; Guo and Santschi 1996; Guo et al. 2000; Rajagopalan and Cheryan 1991). In addition, exposing plankton cells to fresh water can lyse cells, releasing up to 50% of total carbon (Biersmith and Benner 1998).

For these reasons, we chose to use a smaller NMWCO membrane (100 kD) for reduction and diafiltration steps, while maintaining a similar lumen diameter (1 mm), to reduce potential clogging and help to retain any ruptured cell contents. Because DOM in the ocean is strongly weighted toward small size ranges (e.g., Benner and Eadie 1991; Guo et al. 2000), retention of natural DOC was not a major concern. Only 6-7% of total operational DOC has been found to be in the >100 kD HMW fraction (Guo and Santschi 1997a). Further, the little material in this high size range is actually more similar to POC_{susp}, rather than the main DOC pool (Benner et al. 1997; Guo and Santschi 1997b).

We hypothesize that the large observed losses observed stem from the diafiltration step for two reasons: 1) the small surface area of the 100 kD membrane relative to POC concentrations, and 2) the pore sizes were extremely small, in theory greatly reducing chances for fouling. Indeed, we never observed filtration rate changes during reduction. Previous UPOM studies have employed diafiltration using the same membranes and system as for the main filtration, but in contrast to our findings, indicated that losses due to diafiltration are generally small (Benner et al. 1997). Quantitative data on UPOM diafiltration loss has not, however, been previously published. The significantly larger diafiltration losses we observed in our surface samples again suggest that particles here may be more surface active ("sticky"), and/or susceptible to ionic strength changes than mesopelagic samples.

Bacteria and virus retention—Surface water bacteria and virus abundances were determined at 1.2×10^9 and 1.2×10^{10} cells/L, respectively. Mesopelagic bacteria and virus abundances were approximately an order of magnitude lower, 1.3×10^8 and 9.2×10^8 cells/L, respectively. Calculated recoveries of both bacteria and viruses indicated substantial loss occurred during UPOM isolation with all membranes at both depths (Table 5; Fig. 5a). Bacterial recoveries in the main filtration step averaged 25% across all tests (range 14%-42% recovery). High shear tests generally recovered less bacteria and viruses than intermediate shear tests. The fairly large overall ranges observed in the data (Table 5) indicate further testing would be needed to validate such differences. Bacterial counts after reduction were slightly lower than the main filtration, falling to an average of 20% of total source water abundances (range 13%-31%), suggesting only minor additional bacteria losses typically occurred during the reduction step. After diafiltration, bacterial counts were significantly reduced in all tests: final values averaged ~6% of original source bacteria (range 3%-12%). Although counting bacteria in the fresh retentate was somewhat more difficult due to "clumping" (see methods; Fig. 5b), it was still possible to obtain reproducible counts.

Viral abundance results were generally similar to those for bacteria; although larger variability in all recoveries was observed. After the main filtration an average of 35% of viruses were retained relative to source water (range = 14-66%). After reduction (if samples 1 and 2 are considered outliers, since those data only indicate *increases* in viral abundance after reduction), then average viral retention in the salty concentrate averaged 28% (range 4-65%), similar to that observed for bacteria. As with bacteria, diafiltration losses were also very high (~80% relative to salty retentates).

Overall, we conclude that membrane adsorption is also likely the main mechanism for retention of both bacteria and viruses in our system, as has been indicated previously (Benner et al. 1997). This is further supported by the fact that we observed no clear differences in recovery between membrane pore sizes (Fig. 5a), and that average recoveries of both bacteria (25%) and viruses (35%) after the main filtration was generally similar to total POC recoveries, as would be expected for passive loss. Major diafiltration-step losses also appear to occur for both bacteria and viruses, supported by cell aggregation observed in direct counts of diafiltered samples (Fig. 5b).

Elemental and isotopic composition: UPOM vs. GFF—To our knowledge, no published data has directly compared POM composition collected by UF vs. GFF, with the one previous comparison confined to total carbon recoveries (Benner et al. 1997). Our tests suggest that composition effects may in fact exist, with clear offsets in elemental and isotopic values for GFF vs. UPOM. Because our results differ for surface and mesopelagic waters, we treat results for each depth sequentially.

Surface samples—In surface water, our results suggest bulk compositional differences related to both pore size and to GFF data. The 0.1 μm isolated UPOM was more N-rich than the 500 kD UPOM, with average $(C/N)_a$ of 7.3 and 9.7, respectively (Fig. 6b). This offset is very large compared with $(C/N)_a$ variability that we observed in replicates, suggesting real differences. In addition, $\delta^{15}N$ and $\delta^{13}C$ values for 0.1 μm vs. 500 kD membranes were also both consistently offset by 1‰ (Table 4, Fig. 6c,d). Considering the limited number of replicate experiments that were possible, these individual variations cannot be shown to be statistically significant; however, they are both consistent with $(C/N)_a$ ratios in suggesting that the 0.1 μm membrane preferentially isolated a greater proportion of fresh proteinaceous material, partly derived from the N-fixing

Table 5. Bacteria and virus abundance and recovery*

UPOM nr	Depth (m)	Membrane	Step and shear rate	Viruses /L	Viruses %Rec	Bacteria /L	Bacteria %Rec
			Main concentration – H	1.7E+09	14	1.7E+08	14
3	21	500 kD	Reduction	4.8E+08	4	1.8E+08	15
			Diafiltration	1.9E+09	17	4.9E+07	4
			Main concentration – I	3.7E+09	32	5.0E+08	42
4	21	500 kD	Reduction	1.5E+09	13	1.6E+08	13
			Diafiltration	–	–	–	–
			Main concentration – H/I	2.9E+09	25	4.7E+08	40
6	21	0.1 mm	Reduction	1.4E+09	12	1.7E+08	15
			Diafiltration	–	–	–	–
			Main concentration – H	2.6E+08	28	2.1E+07	16
1	674	500 kD	Reduction	8.4E+08	92	2.3E+07	18
			Diafiltration	1.4E+08	15	3.4E+06	3
			Main concentration – I	6.1E+08	66	3.0E+07	23
2	674	500 kD	Reduction	8.4E+08	91	2.9E+07	23
			Diafiltration	1.7E+08	18	1.6E+07	12
			Main concentration – H	2.6E+08	29	2.0E+07	16
7	674	500 kD	Reduction	6.0E+08	65	3.9E+07	31
			Diafiltration	–	–	–	–
			Main concentration – H/I	4.6E+08	50	2.9E+07	23
5	674	0.1 mm	Reduction	4.0E+08	44	2.8E+07	22
			Diafiltration	9.5E+07	10	7.9E+06	6
Source water	21	None	Background concentrations	1.2E+10	100	1.2E+09	100
Source water	674	None	Background concentrations	9.2E+08	100	1.3E+08	100

*Recovery of microbes for each test versus natural seawater abundance. Microbe abundances are given in cell L^{-1} for UPOM samples at three collection stages: initial abundance (main filtration), 100 kD reduction to ~1 L, and 100 kD diafiltration. Bacteria and virus percent recoveries (%Rec) are calculated at each stage relative to source water. H = high shear, I = intermediate shear.

plankton common in this region. Primary production from N-fixation is a major source in this ocean region, at times resulting in $\delta^{15}N$ of fresh POM near 0‰ (Dore et al. 2002; Karl 1999). At the same time, additional proteinaceous material should lead to *both* lower C/N ratios and heavier $\delta^{13}C$, since amino acids are generally ^{13}C enriched relative to other biochemical components (e.g., Degens et al., 1968; Descolasgros and Fontugne 1990). Thus, this explanation is consistent with both expected $\delta^{13}C$ of different biochemical classes, local sources, and finally also with "size-reactivity" continuum ideas (Amon and Benner 1994), which would predict larger material to be less degraded.

Compared with UF, GFF $\delta^{13}C$ values are substantially depleted (by ~3‰) relative to all UPOM samples and also expected marine values (e.g., Karl 1999). Depleted POC $\delta^{13}C$ values relative to typical oceanic plankton $\delta^{13}C$ (–20‰ to –22‰) have also previously been reported in central Pacific UPOM at several sites (Benner et al. 1997; Hernes and Benner 2002; Sannigrahi et al. 2005), and have been interpreted to indicate possible nonmarine C sources delivered via aeolian input. While our depleted surface GFF $\delta^{13}C$ values are squarely in the range, these previous $\delta^{13}C$ values reported from the nearby open ocean, clearly the proximity of our surface water source to an island represents an additional potential source of terrestrial input. Nevertheless, we cannot explain why GFF-POM should have consistently depleted $\delta^{13}C$ values relative to UPOM. This observation suggests the differing mechanisms of particle retention in GFF vs. UF preferentially isolates OM from these waters with strong carbon isotope offsets.

Mesopelagic samples—In contrast with surface samples, mesopelagic isolations showed no obvious compositional differences with pore size (Fig. 6c,d). The $\delta^{13}C$ values averaged –23.5 ± 1.4‰ for all 500 kD isolations and –22.8‰ for the 0.1 μm isolations (Fig. 6c); UPOM $\delta^{15}N$ values from the 500 kD and 0.1 μm experiments averaged +5.7δ ± 1.0‰ and +5.0‰, respectively (Fig. 6d). No clear differences were observed between high or intermediate shear conditions.

Once again, however, there were substantial compositional offsets between UPOM vs. GFF. The average $\delta^{13}C$ for GFF-POM and UPOM differed consistently, with GFF values (–25.7‰)

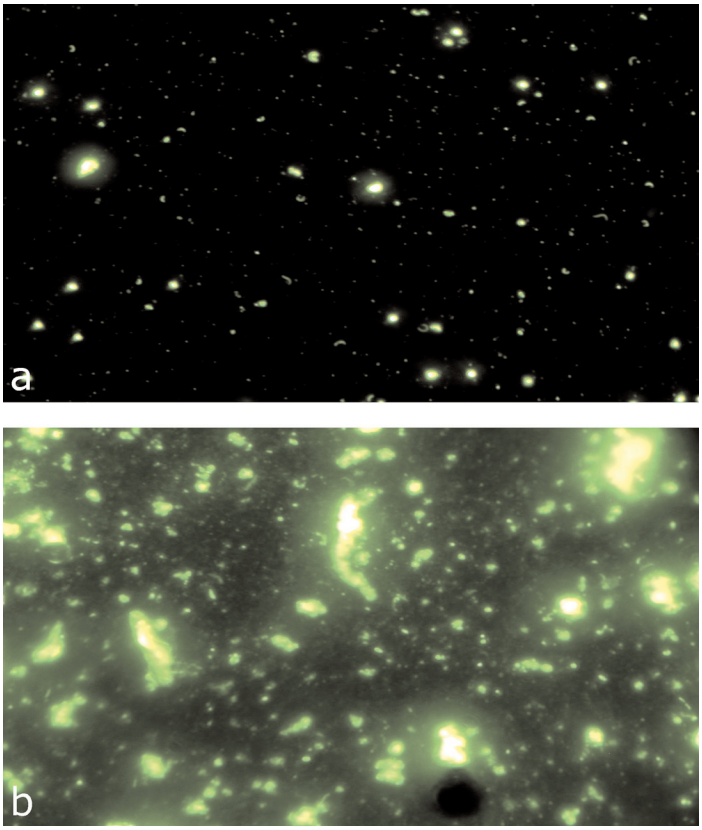

Fig. 5. Bacteria and virus images before and after diafiltration. Micrograph images showing changes in cell distribution, highlighting the clumping of cells due to diafiltration. Sample shown is UPOM #2 (674 m, 500 kD; more details found in Table 1). A) Bacteria (larger cells) and viruses (smaller cells) in seawater matrix after initial concentration step; B) Bacterial aggregate formations observed after diafiltration. A fecal pellet is also visible in panel b.

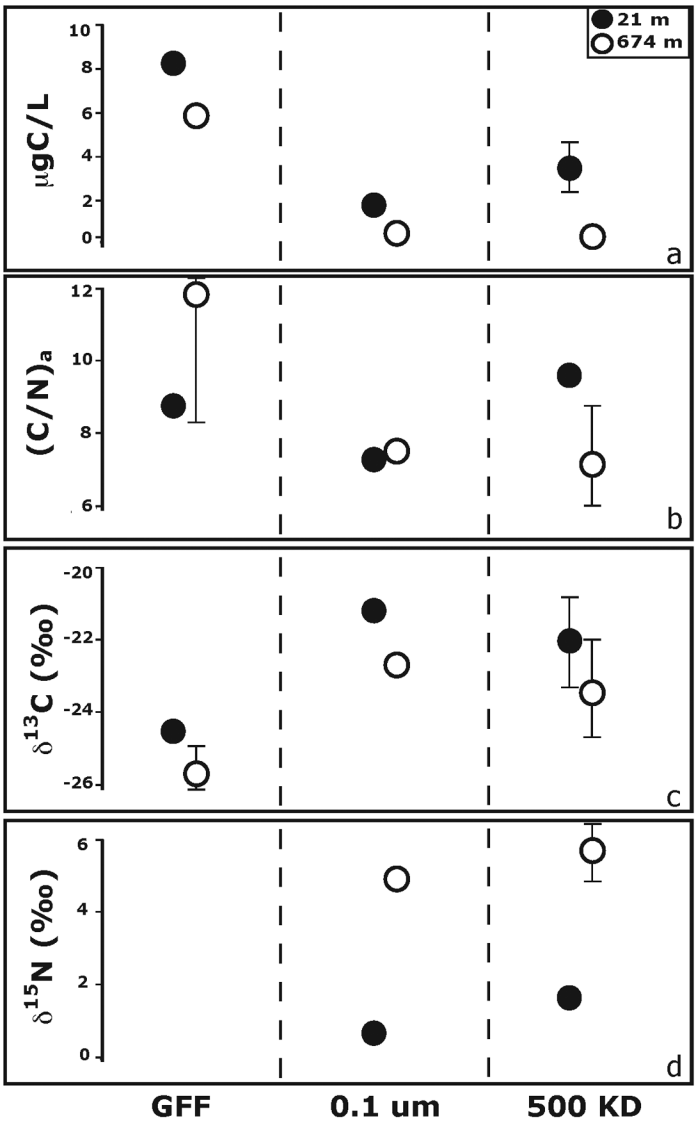

Fig. 6. Average POC concentrations, elemental and stable isotope data for GFF versus UPOM. Data for GFF-POM, 0.1 μm and 500 kD UPOM are compared at 21 m (solid circles) and 674 m (open circles). Error bars represent total ranges; if no error bars are present then range was smaller than size of symbol (except for 0.1 μm membrane samples, where $n = 1$ at each depth). Panels: A) OC concentrations in μg C/L, B) atomic elemental ratios $(C/N)_a$, C) stable carbon isotopic values, $\delta^{13}C$, and D) stable N isotopic values, $\delta^{15}N$; note that GFF filter $\delta^{15}N$ data could not be determined due to insufficient total ON recoveries.

always more depleted than any UPOM sample (–23.4‰), similar to the trend observed in surface waters. Elemental ratios were also strongly offset: GFF-POM also had elevated average $(C/N)_a$ ratios (12.0) relative to UPOM (7.3). Together these comparisons suggest that in deeper water, UF with either pore size preferentially isolated more proteinaceous material than GFF, as enrichment in amino acids would again be consistent with both lower $(C/N)_a$ ratios and heavier $\delta^{13}C$ values.

Comparison with POM_{susp} from offshore Station ALOHA—As a final evaluation of our isolated UPOM, we compared concentration and composition of NELHA samples with literature data on POM_{susp} from the nearby HOT time series site (Station ALOHA). This comparison encompasses not only a general check with previous literature data on UPOM isolations, but also tests the potential of the NELHA water sources, coupled with the ultra-large volume systems we describe, for detailed organic study of POM_{susp} in the Central North Pacific Gyre.

Station ALOHA (22°75′N, 158°10′W) is located approximately 100 km north of Oahu in 4800 m water depth and represents the best-studied reference site for the oligotrophic waters of the north central Pacific gyre (e.g., Karl 1999 and references therein). Long-term averages of GFF-POC concentration at Station Aloha in the upper water column typically fluctuate seasonally between ~1-3 μM OC. The average values we observed in the 21 m source (0.7 μM OC) during our winter sampling are thus consistent with expected lower winter-season values at ALOHA (Karl et al. 1996). This comparison also suggests that POC in the NELHA surface water sources are representative of the truly oceanic waters nearby in terms of

POM, and are not subject to significant OC inputs from coastal or other sources. Observed NELHA elemental ratios are also within typical Station ALOHA ranges (C/N = 5-10), which again vary seasonally (Karl 1999). Deep water POC values are reported less often at station ALOHA, but data indicates that GFF-POC concentrations are ~ 0.5 μM at 350 m, essentially identical to our NELHA 674 m average value of 0.49 μM.

Several studies have also collected UPOM samples from Station ALOHA (Benner et al. 1997; Hernes and Benner 2002; Sannigrahi et al. 2005). Elemental ratios of UPOM isolated during an October sampling period (C/N = 8-10) from the upper water (Sannigrahi et al. 2005) are in the same range as those we report. The prior $\delta^{13}C$ UPOM values (–23.1‰ to –26.5‰) also fall closely in line with our GFF $\delta^{13}C$ values (–24.5‰ to –25.7‰), and are thus somewhat depleted relative to our own UPOM values (–21.8‰ to –23.3‰). While possible reasons for this offset are not clear, we note that both productivity rates and species assemblages at Station ALOHA vary strongly on seasonal and decadal timescales (Karl 1999), so it is possible that variability linked to sampling times influences differences in GFF vs. UPOM material. We also note that the offset in $\delta^{13}C$ evident in our surface and mesopelagic samples is consistent with a general trend toward lighter $\delta^{13}C$ UPOM values with increasing depth that has been reported both at Station ALOHA (Hernes and Benner 2002; Sannigrahi et al. 2005), and also in the oligotrophic Atlantic (Hernes and Benner 2006).

Finally, surface Station ALOHA measurements of GFF-POM $\delta^{15}N$ values vary between about –1‰ and +1‰ yearly; more positive surface values are observed in winter, while deeper water values (>175 m) remain more constant near +5‰ (Dore et al. 2002). To our knowledge there are no published UPOM $\delta^{15}N$ values from any nearby waters. We measured increasing $\delta^{15}N$ values with depth (+1.5‰ at 21 m to +5.5‰ at 674 m), values correspond very closely with $\delta^{15}N$ of GFF-POM at Station ALOHA (Fig. 6d; Dore et al. 2002). This suggests that, at least during this winter season time period, the relative input of PON from N-fixation at NELHA was also very similar to what is observed at ALOHA.

Discussion

The home-built design we have described fully met our main objectives: a relatively low-cost, easy-to-assemble system that can act as an effective replacement for systems that are no longer available, or as an alternative to cost-prohibitive commercial instruments. It proved efficient in the collection of large amounts of POM_{susp} during a reasonable timeframe, resulting in no observable cell damage or lysis, even at high shear with larger and more delicate phytoplankton species. Specific aspects of POM_{susp} concentration, including recoveries, retention of microbes, and bulk composition compare well with previous UPOM data. Our design also provides significant flexibility in configuration, membranes, and ultimate processing rate. We directly tested a number of aspects of UPOM isolation that have not previously been investigated, such as effects of shear rate, pore-size effects, effect of long recycle times, and bulk composition relative to GFF. The ultra-large volumes of POM_{susp} that can be processed using our two-stage approach substantially expands the breadth of experiments that could be done in the future on this very important but relatively less-studied oceanic carbon reservoir. Novel but highly sample intensive analyses, such as compound-specific isotope measurements or solid state NMR, can now be readily applied.

Coupling our ultra-large volume design with the NELHA sampling site underlines an opportunity to study sample-intensive aspects of POM_{susp} in the oligotrophic ocean. A number of papers on both POM and DOM have already been published using the NELHA water sources (e.g., Ingalls et al. 2006; Repeta and Aluwihare 2006), and other projects are ongoing. Our study is the first to present a detailed elemental and isotopic data set on POM from the NELHA station water sources, and make a direct comparison with nearby open ocean sites. The favorable comparison to station ALOHA data suggests that the essentially unlimited volumes of surface and mesopelagic water available at NELHA represents an unparalleled opportunity to study central North Pacific gyre organic matter without ship time.

One important aspect for interpretation of both future and past POM work is that our data suggests that both filtration method (GFF vs. UF), and membrane pore size (in surface water), may lead to compositional variation in isolated material. In more particle-rich surface waters, the offsets in composition that we observed with different membrane pore sizes generally corresponded to size-reactivity ideas (Amon and Benner 1994); material retained with larger pore sizes was more N-rich, with corresponding expected shifts in elemental and isotopic values. In mesopelagic water, pore-size related offsets were not observed, perhaps because POM_{susp} is much more degraded and homogenous.

Substantial composition offsets in UPOM vs. GFF-POM were observed at all depths, but are more difficult to interpret. In principle, decreasing in nominal pore size from GFF (~0.7 μm) to 0.1 μm to 500 kD represents a clear size progression. However, even in surface waters, we did not observe consistent trends in all compositional values from GFF to smaller UPOM. We hypothesize that this is most likely due to the fundamentally different mechanism of POM retention. GFF filters retain material by clogging and adsorption, and some studies have indicated that GFF filters may actually adsorb an important portion of DOM and colloidal material pools (Moran et al. 1999). Compositional offsets due to losses via adsorption in UPOM systems are also possible, although evidence for CPP layer formation as the main loss mechanisms suggests this is less likely, it should be investigated. Overall, UPOM collection appears prone to under-sampling total material, with possible compositional offsets based on pore size used; in contrast, GFF filters may be prone to some over-sampling, with possible compositional effects linked to inclusion of compositionally

distinct dissolved materials. These results suggest caution in attempting to directly compare detailed composition in GFF vs. UPOM samples.

Comments and recommendations

Based on our tests we offer the following general recommendations for system configuration and operation.

Membrane pore size—We would generally recommend using the 0.1 μm, at least in oceanic (low-POC) waters. Flow rates are much faster with the larger pore size, increasing throughput substantially, while neither fouling behavior, final carbon recovery, or retention of microbes differed greatly between 500 kD nor 0.1 μm pore sizes. However, in eutrophic or particle rich waters where fouling may become an important issue, the 500 kD membrane could provide important advantages.

Membrane surface area—Membrane surface area presents a tradeoff between permeate flow rate and carbon loss, since our data indicate carbon loss is primarily due to adsorption via the CPP mechanism. The relatively large surface area membranes we used may be one explanation for our lower *relative* recoveries vs. GFF. We thus recommend choosing membrane size (surface area) based on target volumes. If total volumes are relatively small (<1000 L) then larger surface area membranes such as those we used may actually lead to lower recoveries. With very large volumes, the *total* amount of material ultimately recovered (not the percentage) will quickly make up for membrane adsorption.

Shear rate conditions—We recommend using high shear conditions because we observed no cell damage and noticed insignificant differences in final recovery and fouling behavior.

Losses due to diafiltration and microbial contribution to UPOM—We observed large losses of material due to diafiltration in surface waters. Recoveries of bacteria and viruses seemed especially susceptible to loss with decreasing ionic strength. In studies involving desalting where microbial contributions are of interest, losses due to diafiltration should be carefully investigated. It would also be useful to investigate the mechanism of these losses, e.g., either clumping and adsorption to the membrane surface or passage of lysed or disaggregated material into the diafiltration permeate.

UPOM vs. GFF-POM composition—We advise collecting GFF samples in tandem with UF processing in any study for which tying UPOM results back to the larger GFF literature is of interest, to at least establish any offsets in bulk properties for a given water mass.

UF as a tool for studying phytoplankton assemblages—The fact that delicate cells remained intact and at high concentration factors suggests that relatively rare new species might be identified by plankton biologists, and species occurring at low abundance in oceanic regions might be more accurately counted using this approach.

References

Alldredge, A. L., and G. A. Jackson. 1995. Aggregation in marine systems - Preface. Deep-Sea Res. II 42:1-7.

Altmann, J., and S. Ripperger. 1997. Particle deposition and layer formation at the crossflow microfiltration. J. Membrane Sci. 124:119-128.

Amersham Biosciences. 2004. Operating guide for hollow fiber cartridges and systems. GE Healthcare (USA).

Amon, R. M. W., and R. Benner. 2004. Rapid cycling of high-molecular-weight dissolved organic matter in the ocean. Nature 369:549-552.

Bauer, J. E., and E. R. M. Druffel. 1998. Ocean margins as a significant source of organic matter to the deep ocean. Nature 392:482-485.

Benner, R., B. Biddanda, B. Black, and M. McCarthy. 1997. Abundance, size distribution, and stable carbon and nitrogen isotopic compositions of marine organic matter isolated by tangential-flow ultrafiltration. Mar. Chem. 57:243-263.

——— and B. J. Eadie. 1991. Isolation by ultrafiltration of a new component of dissolved organic-matter. Abstracts of Papers of the American Chemical Society 201.

Biersmith, A., and R. Benner. 1998. Carbohydrates in phytoplankton and freshly produced dissolved organic matter. Mar. Chem. 63:131-144.

Bird, R. B., W. E. Stewart, and E. N. Lightfoot. 1960. Transport phenomena. Wiley.

Bishop, J. K. B., J. M. Edmond, D. R. Ketten, M. P. Bacon, and W. K. Silker. 1977. The chemistry, geology, and vertical flux of particulate matter from the upper 400 m of the equatorial Atlantic Ocean. Deep-Sea Res. I 24:511-548.

Cheryan, M. 1998. Ultrafiltration and microfiltration handbook. Technomic Publishing Comp.

Clegg, S. L., M. P. Bacon, and M. Whitfield. 1991. Application of a generalized scavenging model to thorium isotope and particle data at equatorial and high-latitude sites in the Pacific Ocean. J. Geophys. Res. Oceans 96:20655-20670.

Degens, E. T., and others. 1968. Metabolic fractionation of carbon isotopes in marine plankton, II. Data on samples collected off the coasts of Peru and Ecuador. Deep Sea Res. II 15:11-20.

Descolasgros, C., and M. Fontugne. 1990. Stable carbon isotope fractionation by marine-phytoplankton during photosynthesis. Plant Cell Environ. 13:207-218.

Dore, J. E., J. R. Brum, L. M. Tupas, and D. M. Karl. 2002. Seasonal and interannual variability in sources of nitrogen supporting export in the oligotrophic subtropical North Pacific Ocean. Limnol. Oceanogr. 47:1595-1607.

Druffel, E. R. M., S. Griffin, J. E. Bauer, D. M. Wolgast, and X. C. Wang. 1998. Distribution of particulate organic carbon and radiocarbon in the water column from the upper slope to the abyssal NE Pacific ocean. Deep-Sea Res. II 45:667-687.

Ghaffour, N. 2004. Modeling of fouling phenomena in cross-flow ultrafiltration of suspensions containing suspended solids and oil droplets. Desalination 167:281-291.

Guo, L. D., C. H. Coleman, and P. H. Santschi. 1994. The distribution of colloidal and dissolved organic-carbon in the Gulf of Mexico. Mar. Chem. 45:105-119.

——— and P. H. Santschi. 1996. A critical evaluation of the cross-flow ultrafiltration technique for sampling colloidal organic carbon in seawater. Mar. Chem. 55:113-127.

——— and ———. 1997a. Composition and cycling of colloids in marine environment. Rev. Geophys. 35:17-40.

——— and ———. 1997b. Isotopic and elemental characterization of colloidal organic matter from the Chesapeake Bay and Galveston Bay. Mar. Chem. 59:1-15.

———, L. S. Wen, D. G. Tang, and P. H. Santschi. 2000. Re-examination of cross-flow ultrafiltration for sampling aquatic colloids: evidence from molecular probes. Mar. Chem. 69:75-90.

Hasle, G. R. 1978. The inverted microscope method. Monographs oceanogr. methodol. 6:88-96.

Hedges, J. I., and J. H. Stern. 1984. Carbon and nitrogen determinations of carbonate-containing solids. Limnol. Oceanogr. 29:663-666.

Hernes, P. J., and R. Benner. 2002. Transport and diagenesis of dissolved and particulate terrigenous organic matter in the North Pacific Ocean. Deep-Sea Res. I 49:2119-2132.

——— and ———. 2006. Terrigenous organic matter sources and reactivity in the North Atlantic Ocean and a comparison to the Arctic and Pacific oceans. Mar. Chem. 100:66-79.

Hobbie., J. E., R. J. Daley, and S. Jasper. 1977. Use of nuclepore filters for counting bacteria by fluorescence microscopy. Appl. Environ. Microbiol. 1225-1228.

Hong, S., R. S. Faibish, and M. Elimelech. 1997. Kinetics of permeate flux decline in crossflow membrane filtration of colloidal suspensions. J. Colloid Interface Sci. 196:267-277.

Ingalls, A. E., and others. 2006. Quantifying archaeal community autotrophy in the mesopelagic ocean using natural radiocarbon. Proc. Nat. Acad. Sci. U.S.A. 103:6442-6447.

Jaffrin, M. Y., L. H. Ding, C. Couvreur, and P. Khari. 1997. Effect of ethanol on ultrafiltration of bovine albumin solutions with organic membranes. J. Membrane Sci. 124:233-241.

Karl, D. M. 1999. A sea of change: Biogeochemical variability in the North Pacific Subtropical Gyre. Ecosystems 2:181-214.

——— and others. 1996. Seasonal and interannual variability in primary production and particle flux at Station ALOHA. Deep-Sea Res. I 43:539-568.

Lee, C., S. G. Wakeham, and C. Arnosti. 2005. Particulate organic matter in the sea: The composition conundrum. Ambio 33:565-575.

———, S. G. Wakeham, and J. I. Hedges. 2000. Composition and flux of particulate amino acids and chloropigments in equatorial Pacific seawater and sediments. Deep-Sea Res. I 47:1535-1568.

McCave, I. N. 1984. Size spectra and aggregation of suspended particles in the deep ocean. Deep-Sea Res. A 31:329-352.

McNichol, A. P., and L. I. Aluwihare. 2007. The power of radiocarbon in biogeochemical studies of the marine carbon cycle: Insights from studies of dissolved and particulate organic carbon (DOC and POC). Chem. Rev. 107:443-466.

Megens, L., J. vanderPlicht, J. W. deLeeuw, and F. Smedes. 2002. Stable carbon and radiocarbon isotope compositions of particle size fractions to determine origins of sedimentary organic matter in an estuary. Org. Geochem. 33:945-952.

Minor, E. C., T. I. Eglinton, R. Olson, and J. J. Boon. 1998. The compositional heterogeneity of particulate organic matter from the surface ocean: an investigation using flow cytometry and DT-MS. Organic Geochem. 29:1561-1582.

Moran, S. B., M. A. Charette, S. M. Pike, and C. A. Wicklund. 1999. Differences in seawater particulate organic carbon concentration in samples collected using small- and large volume methods: the importance of DOC adsorption to the filter blank. Mar. Chem. 67:33-42.

Noble, R. T., and J. A. Fuhrman. 1998. Use of SYBR Green I for rapid epifluorescence counts of marine viruses and bacteria. Aquat. Microb. Ecol. 14:113-118.

Powell, M. J., and A. T. Timperman. 2005. Quantitative analysis of protein recovery from dilute, large volume samples by tangential flow ultrafiltration. J. Membrane Sci. 252:227-236.

Rajagopalan, N., and M. Cheryan. 1991. Total protein isolate from milk by ultrafiltration - factors affecting product composition. J. Dairy Sci. 74:2435-2439.

Repeta, D. J. 1984. Transformation reactions and recycling of carotenoids and chlorins in the Peru upwelling region. Geochim. Cosmochim. Acta 48:1265-1277.

———, and L. I. Aluwihare. 2006. Radiocarbon analysis of neutral sugars in high-molecular-weight dissolved organic carbon: Implications for organic carbon cycling. Limnol. Oceanogr. 51:1045-1053.

Sannigrahi, P., E. D. Ingall, and R. Benner. 2005. Cycling of dissolved and particulate organic matter at station Aloha: Insights from C-13 NMR spectroscopy coupled with elemental, isotopic and molecular analyses. Deep-Sea Res. I 52:1429-1444.

Shaw, T. J., J. M. Smoak, and L. Lauerman. 1998. Scavenging of ex(234)Th, ex(230)Th, and ex(210)Pb by particulate matter in the water column of the California Continental Margin. Deep-Sea Res. II 45:763-779.

Song, L. F., and M. Elimelech. 1995. Theory of concentration polarization in cross-flow filtration. J. Chem. Soc. Faraday Trans. 91:3389-3398.

Suess, E. 1980. Particulate organic carbon flux in the oceans - surface productivity and oxygen utilization. Nature 288:260-263.

Utermöhl, H. 1958. Zur Vervollkommnung der quantitativen Phytoplankton Methodik. Mitt. Int. Theor. Angew. Limn. 9:1-38.

Wakeham, S. G., and E. A. Canuel. 1988. Organic geochemistry of particulate matter in the eastern tropical North Pacific Ocean: implications for particle dynamics. J. Mar. Res. 46:183-213.

——— and J. R. Ertel. 1988. Diagenesis of organic-matter in suspended particles and sediments in the Cariaco Trench. Organic Geochem. 13:815-822.

———, C. Lee, J. I. Hedges, P. J. Hernes, and M. L. Peterson. 1997. Molecular indicators of diagenetic status in marine organic matter. Geochim. Cosmochim. Acta 61:5363-5369.

Zeman, L., and L. Denault. 1992. Characterization of microfiltration membranes by image-analysis of electron-micrographs. 1. Method development. J. Membrane Sci. 71:221-231.

Submitted 9 October 2007
Revised 21 October 2008
Accepted 15 November 2008